



# Control of Quasi Z-Source Converter in a Microgrid Using Modified Power Ratio P&O MPPT

Ch. Sreenu<sup>1</sup>(✉), G. Mallesham<sup>1</sup>, and T. Chandra Shekar<sup>2</sup>

<sup>1</sup> Department of Electrical Engineering, University College of Engineering, Osmania  
University, Hyderabad, India

chsreenu245@gmail.com, drgm@osmania.ac.in

<sup>2</sup> Department of Electrical Engineering, Maturi Venkata Subba Rao Engineering College,  
Hyderabad, India

**Abstract.** In this paper, a quasi-Z-source inverter (QZsi) is used to model and regulate a hybrid photovoltaic (PV) wind microgrid. This inverter has significant advantages over conventional inverters, including superior buck/boost characteristics, high power performance features, a lack of filter requirement, lower harmonic contents, and the ability to control phase angle output. To maintain high voltage, gain during maximum power point tracking (MPPT) operations, as DC-DC switching power equipment, a SEPIC converter is employed. The suggested controller combines distributed generation (DG) with loads effectively and operates with battery systems, wind turbines, and hybrid PV under a variety of operational situations. Only rural areas can use the recommended freestanding microgrid technology. Using MATLAB Simulink, the proposed microgrid system has been tested under a variety of load-cutting, solar, wind, and environmental conditions. The results of the studies which were run on Simulink, demonstrate that a microgrid with QZsi architecture can function successfully in this situation.

**Keywords:** SEPIC converter · Maximum Power Point (MPP) · QZsi · Maximum Power Ratio Variable Step (MPRVS) · PV · Switched Mode Power Converter (SMPC)

## 1 Introduction

Traditional fossil fuel-based power generation is rapidly declining as a result of the adverse effects of excessive carbon emissions on the environment [1]. To meet the growing energy demand, the concept of a microgrid has emerged as a practical action to integrate the use of sources of environmentally friendly energy into every existing power grid. Additionally, transmission lines' power loss was decreased and distribution systems' power flow was improved [2]. The primary goal of the microgrid is to use RES, such as more closely spaced Photovoltaic (PV), Wind Turbine Generator (WTG), and Energy Storage Systems (ESS) systems, to deliver high-quality, dependable electricity to a sensitive legion. Depending on the micro-grid, built as alternating current networks

or direct current networks because loads need pair alternating current and direct current power. To satisfy the load supply requirements, multiple methods for changing power from alternating current to direct current or conversely are needed. Every inefficient and unreliable method of using multiple power electronic converters results in harmonic interactions in the system [3]. Alternating current microgrids act as common since they can provide a variety of DG components and weights. The main drawbacks are DG unit synchronizing and circulating harmonic currents are requirements of a Microgrid [4]. Reactive power does not exist in DC microgrids because of the absence of a requirement to coordinate the distribution system. Moreover, grid controllers are increasingly drawn to Direct Current microgrids because DC loads powered by renewable energy sources become more widely used [5]. Due to the significant changes that must be made to power networks to integrate DC microgrids into distribution networks, it is a pricey choice [6]. Thus, mixed microgrids are a great option for incorporating tiny grids with distinct while reducing conversion losses, DG, and load types that can be integrated into conventional power systems [7]. Integrating converters (ICs) are utilized to couple direct-current and alternate-current sub-grids. Typically, a regular VSI is utilized, but a step-up stage is needed to deliver a suitable voltage for regarding the network. The outcome is its strategy boosts the price as well as conversion capacity reducing the devices' performance and dependability [8]. A qZSC is incorporated into a sustainable microgrid to address this problem. Reduced voltage strain, stable input currents, and similar grounding of the Dc supply make the qZSC more advantageous for Photovoltaic systems [9]. The not-magnetically linked Z source conversion (ZSC), which includes the qZSC, that was presented as [10], is described in terms of its operating modes. Researchers have also looked into the inverter's modeling and analysis [11]. Several studies that concentrate on renewable energy-based systems have used a qZSC [12–14]. Although it was more focused on energy storage control, qZSC also is utilized [15] as an integrated circuit in a mixed AC/DC microgrid. Implementing the qZSC and its control mechanisms in renewable hybrid microgrids still takes a lot of work despite their advantages. In this work, the functional dependability and energy requirements of a renewable microgrid are addressed by a DC and AC sub-grid with renewable energy sources via a QZSC. Running the hybrid microgrid requires system configuration. A PV array is used as Distributed generation along with DC loads in the DC sub-grid, whereas a wind farm unit is used as DG along with Electrical loads in the AC sub-grid. The Z-Source Quasi inverter used in the inverter, which is connected to the wind- PV DC-DC boost converter, has better step-down/step-up characteristics, can regulate the continuous running mode of operation, which results in a lower harmonic content, higher efficiency, and better power performance [16]. Using only a simulation environment (MATLAB), this paper discusses how microgrids behave under various loading situations, solar insolation, wind speed, and diesel generator scenarios. In this study, a hybrid PV-Wind diesel with a QZSI has been used to decrease the number of reverse conversions and increase the effectiveness of the microgrid. Additionally, the SEPIC DC-DC converter functions as a direct current link interface for maximum power point tracking.

## 2 Proposed Method

The structure of a proposed microgrid using a QZSI for development with a renewable energy source is shown in Fig. 1. A storage device, a power electronic converter, a PV generator, and various topologies of wind turbines make up the microgrid system. A turbine is mechanically connected to the rotation of a wind farm. In an equivalent circuit with a single-diode model to generate electricity because it has a greater power extraction capacity than that model. Its characteristics can be used to approximate the aerodynamic torque or power despite being a sophisticated wind turbine device. Moreover, a storage solution is needed to equalize the random variations of PV and wind electricity provided to the network. The modeling procedure used to produce these essential components of the proposed wind-PV system is briefly described in this section.

### 2.1 Diesel Generator

In reality, a diesel generator is a device that transforms mechanical energy produced by a combustion engine built right into the machine into electrical energy. The diesel generator's various parts all function together to generate electricity. An engine that runs on diesel is found inside a diesel generator. To be used during power outages, the mechanical energy that is produced is further transformed into electrical energy.

### 2.2 Quasi-Z Source Converter (QZSC)

Figure 2 depicts the main architecture of the 1-ph QZSC.

Based on the circuit layout of Fig. 3, whenever the qZSI is in a short-circuit position for a period of  $T_{sh}$  following the switching period of  $T$ . The subsequent equations are written.

$$V_{in} + V_{C2} = V_{L1}; V_{out} = 0 \quad (1)$$

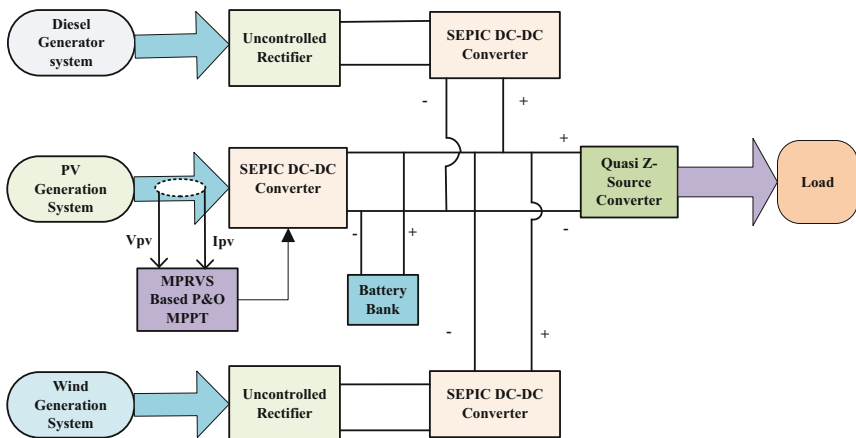
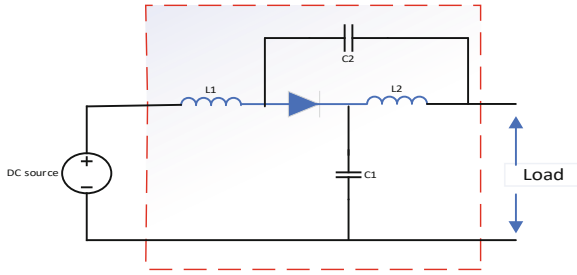


Fig. 1. Block diagram with the structure of the microgrid.



**Fig. 2.** Basic model of Quasi Z-Source converter.

when the Qzsi is an active state condition for the time of  $T_{nsh}$  from the switching period of  $T$ , the formula is.

$$V_{L1} = V_{in} - V_{C1} = V_{in} - V_{out} + V_{C2} \tag{2}$$

$$V_{L1} = V_{C1} - V_{out} = V_{C2} \tag{3}$$

Since a mean coil potential for a switching period has ended under a steady state, from Eqs. 1 and 3, we obtain

$$V_{L1} = \frac{T_{sh}(V_{in} + V_{C2}) + T_{nsh}(V_{in} - V_{C1})}{T} = 0 \tag{4}$$

$$V_{L2} = \frac{T_{sh}(V_{C2}) + T_{nsh}(-V_{C1})}{T} = 0 \tag{5}$$

Consequently

$$V_{C1} = \frac{T_{nsh}}{T_{nsh} - T_{sh}} V_{in} \text{ and } V_{C2} = \frac{T_{sh}}{T_{nsh} - T_{sh}} V_{in} \tag{6}$$

Quasi-Z-source dc-dc converters can generate both positive and negative polar step-down step-up voltages thanks to a unique LC impedance network. There are some MPPT approaches available, including better perturbation and observation (P&O) techniques (IP&O). The easiest way is P&O, which gradually raises or lowers the voltage of the PV array while moving a running point located in the path of the peak power level.

### 2.3 PV System

The most well-known method of using solar energy is through PV installations, which transform solar energy into electrical energy. As semiconductor devices, solar photovoltaic cells share many processing and manufacturing processes with other semiconductor devices like computers and memory chips. The standards for semiconductor device purity and quality control are quite stringent, as is well known.

Using Kirchhoff’s current law for current, the governing equation for this equivalent circuit is created.

$$I = I_L - I_D - I_{sh} \tag{7}$$

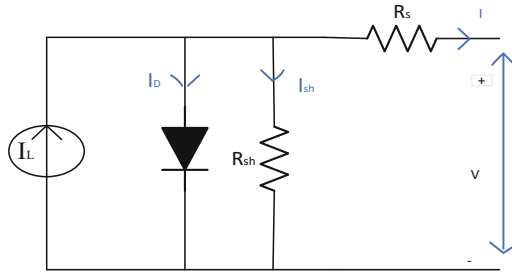


**Fig. 3.** Circuit for a PV cell.

$I_D$  Shockley's is modeled by the typical semiconductor equation.

$$I_D = I_0 \left[ \exp\left(\frac{V + IR_S}{\eta V_T}\right) - 1 \right] \quad (8)$$

$V_T$  thermal voltage given by:

$$V_T = \frac{kT_C}{q} \quad (9)$$

Therefore, the complete single-diode model is:

$$I = I_L - I_0 \left[ \frac{V + IR_S}{\eta V_T} - 1 \right] - \left[ \frac{V + IR_S}{R_{sh}} \right] \quad (10)$$

## 2.4 Wind System

Today, electricity is primarily produced using wind energy. The atmospheric pressure gradients that cause wind cause air to move. The wind blows in a direction from upper to lower pressure. The greater the wind speed, the greater amount of wind energy that can be converted into usable power by utilizing energy-conversion equipment. The production and movement of wind are complex processes brought on by several variables. Wind energy is the method for harnessing wind-generating energy. Wind energy resource that regulates the wind's overall strength.

**Wind power is given by**

$$P = \frac{1}{2} \rho A V^3 \quad (11)$$

where,

P = Power,  $\rho$  = Air density, A = Swept area of blades given by  $A = \pi r^2$ .

Where r is the radius of the blades and V is the Velocity of the wind.

### 2.5 SEPIC Converter Design

Every dc-dc converter quickly turns on and off a switch, usually with a high-frequency pulse. Because of what it achieves, as a result, the SEPIC converter is superior. In the SEPIC, L1, and C1 are charged by the incoming volts when the switch is activated and the pulse is high. C2 keeps the output even when the diode was out. The coils output through the diode to the load and charge the batteries when the toggle also isn't activated. In proportion to how much output will increase during periods of a low pulse. This occurs from the inductors' voltage increasing as the charge lasts longer. As shown in Fig. 4, If the signal lasts too long, the batteries won't be capable of charging, and the converter will quit functioning.

The final equation's ideal Dc-dc conversion is provided by.

$$V_0 = \frac{D * V_i}{1 - D} \tag{12}$$

Losses brought on by parasitic elements like the diode drop  $V_D$  are not taken into account by this, though.

Therefore

$$V_0 + V_D = \frac{D * V_i}{1 - D} \tag{13}$$

From Eq. (13)

$$D = \frac{V_0 + V_D}{V_0 + V_i + V_D} \tag{14}$$

When the input voltage is at its lowest, the Duty Cycle will be at its highest. The highest Duty cycle is

$$D_{max} = \frac{V_0 + V_D}{V_0 + V_{i\min} + V_D} \tag{15}$$

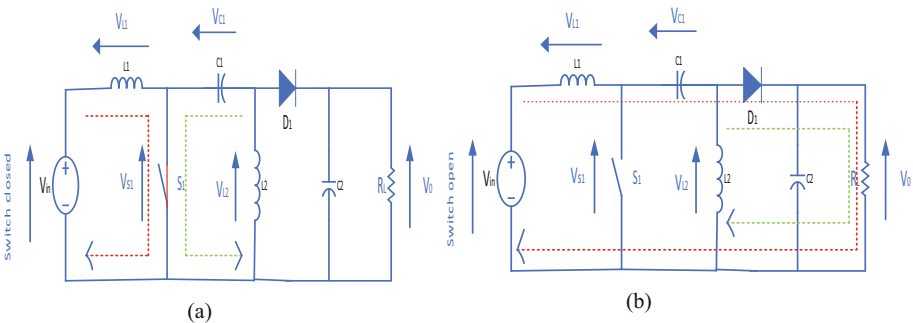


**Fig. 4.** (a) Sepic converter switch is closed. (b). The Sepic converter switch is open.

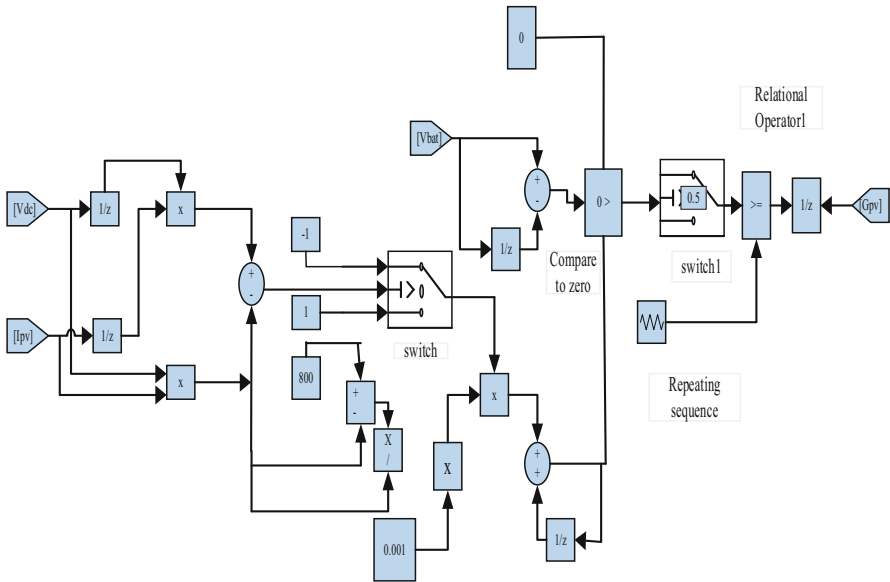


Fig. 5. MPRVS-based P&O technique control model.

### 3 Step-Based P&O MPPT with Modified Power Ratio

Figure 5 depicts a prototype for the P&O method based on MPRVS for the best extraction of sun module-derived Photovoltaic energy. Without the assistance of the PI controller, the SEPIC converter can generate gating pulses, which force the operating point to be close to the MPP and reduces power oscillation. Additionally, it guards against overvoltage in the battery charging system.

### 4 Results and Discussion

Using P&O MPPT based on MPRVS and a quasi-Z-source inverter, the proposed hybrid PV-Wind-Diesel generator microgrid is tested. The proposed hybrid microgrid's developed structure, which is based on MATLAB Simulink, is shown in Fig. 1. The maximum power ratio variable step-based P&O MPPT voltage and current sensors, which are used to measure the Photovoltaic panel parameters,  $V_{pv}$  and  $I_{pv}$ , respectively, are what drive the SEPIC converter. A synchronous generator with a permanent magnets-based wind emulator system is utilized as the wind turbine generator. By altering the wind turbine's characteristics, the wind turbine's speed changes as a result of the SMPC, producing the necessary physical force.

As can be seen in Fig. 6a, various wind operating conditions were used to test the precision of the suggested modified power ratio-based Perturb and observe maximum power point. The employed controller, which is operational in the maximum power region, provides the best wind power tracking during the abrupt changes in the wind speed depicted in Fig. 6b. The associated rate of duty for the Sepic constant current converter

is shown in Fig. 6c. Additionally, the ability of the suggested maxim power point tracker is evaluated beneath early pioneer’s scenario accompanied by stage sunlight. Figure 6d is diesel generator power. Figure 7 shows that the propped system has acquired values for the Photovoltaic system under the phase variations in direct solar radiation, and has proven to be highly accurate and effective at tracking PV in the MPP region. Figure 8 illustrates how the recommended hybrid microgrid performs underneath the next set of circumstances, which include changing wind speeds and constant solar radiation. Figure 9 displays the utility’s reaction side to various wind speeds and constant radiation from the sun. Figure 10 also illustrates the performance of the microgrid below conditions of changing sun rays and persistent wind speed when modified power ratio-based Perturb and observe MPPT is used. Figure 11 illustrates the performance of diesel generators under load-cutting conditions. Figures 12 and 13 (a) & (b) depict the based scheme microgrid accurate efficiency across different working scenarios (detaching operating conditions from the microgrid and then re-connecting operating conditions energies to the microgrid, respectively). Under operating conditions where the wind generator is disconnected from and reconnected to the microgrid, its performance is assessed. The Sim Power Systems toolkit has been used to build the entire set of version gadgets. The simulation parameters applied to the created B2B QZS-integrated hybrid model in Table 1 show how the desired outcome was achieved.

**Table 1.** Simulation parameters.

| QZS Parameters           |                |                      | SEPIC converter parameters |                |        |
|--------------------------|----------------|----------------------|----------------------------|----------------|--------|
| Inductor and capacitors  | L <sub>1</sub> | 1mH                  | Capacitor                  | C <sub>1</sub> | 3.5mF  |
|                          | L <sub>2</sub> | 1mH                  | Inductance                 | L1             | 0.42mH |
|                          | C <sub>1</sub> | 1 μF                 | Output capacitor           | C2             | 3.5mF  |
|                          | C <sub>2</sub> | 1 μF                 | Inductance                 | L2             | 0.42mH |
| Wind-Solar/PV parameters |                |                      | Diesel generator           |                |        |
| PV: Open circuit voltage | Voc            | 33.53V               | Nominal power              | Pn (VA)        | 1kVA   |
| Short circuit current    | Isc            | 8.24A                | line-to-line voltage       | Vn(Vrms)       | 200V   |
| Operating Temp           | T              | 35 °C                | frequency                  | fn (Hz)        | 50Hz   |
| Irradiation              | S              | 1000W/m <sup>2</sup> |                            |                |        |
| Pv Power                 | Ppv            | 200W                 |                            |                |        |
| Wind power               | Pwind          | 150W                 |                            |                |        |



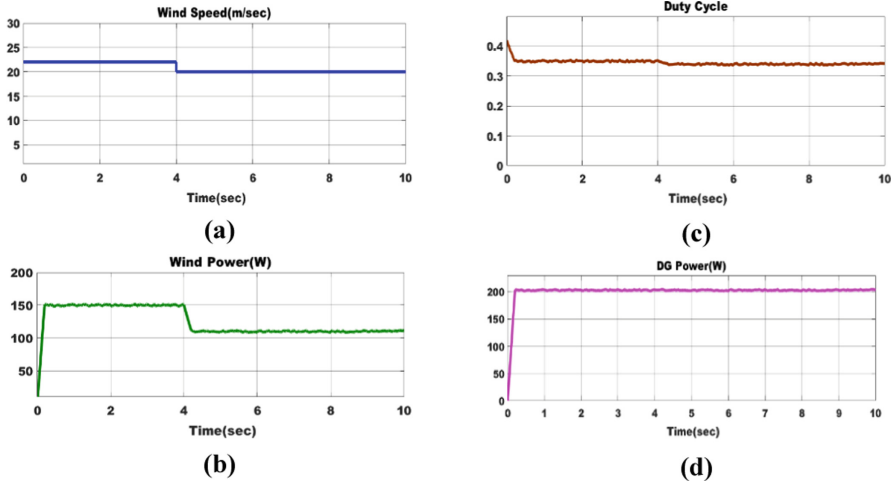


**Fig. 6.** Simulation results (a) Wind speed changed abruptly (b) Power wind, and (c) Sepic converter duty factor (d) Diesel generator power.

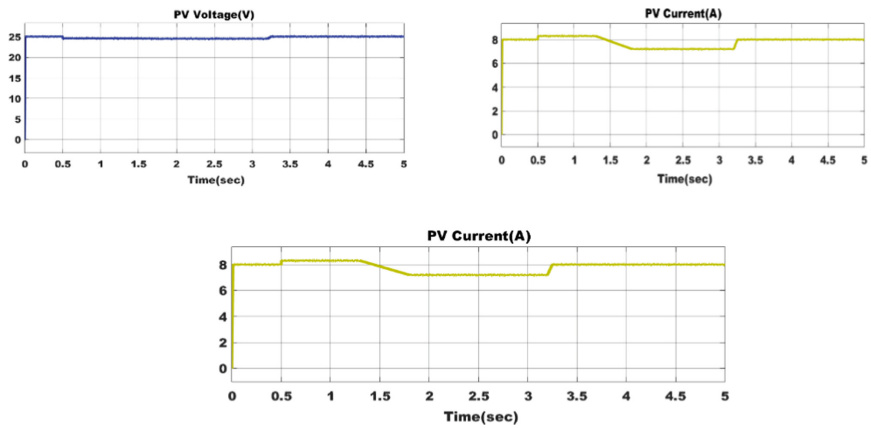


**Fig. 7.** Responses of PV systems to solar irradiation changes.

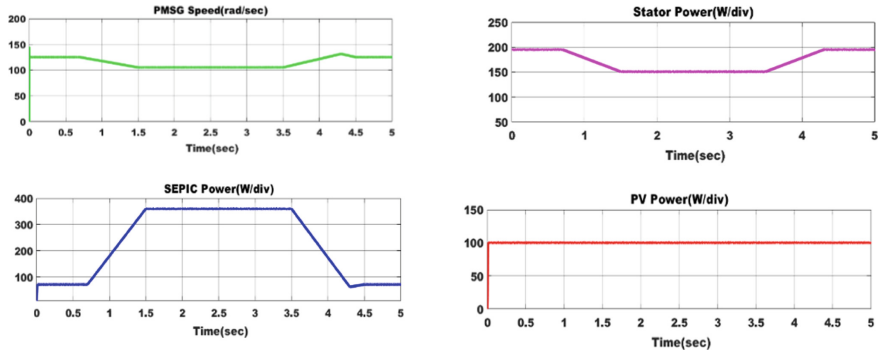


**Fig. 8.** The ability of the suggested hybrid microgrid under shifting wind conditions and constant sunlight.

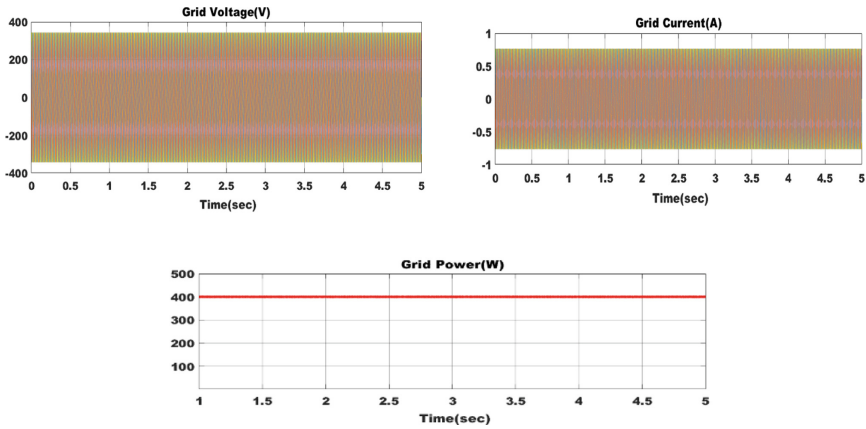


**Fig. 9.** Grid Side Response with Varying Wind Speed and Constant Sunlight.

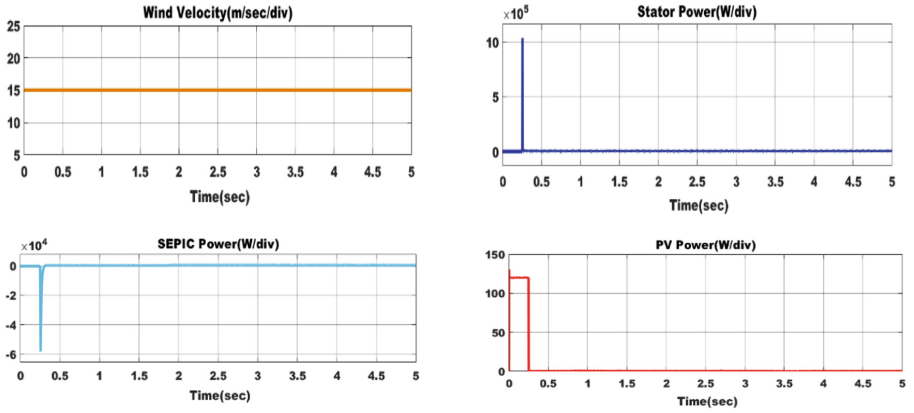


**Fig. 10.** The hybrid microgrid's behavior responds to solar radiation variation and steady wind speed.

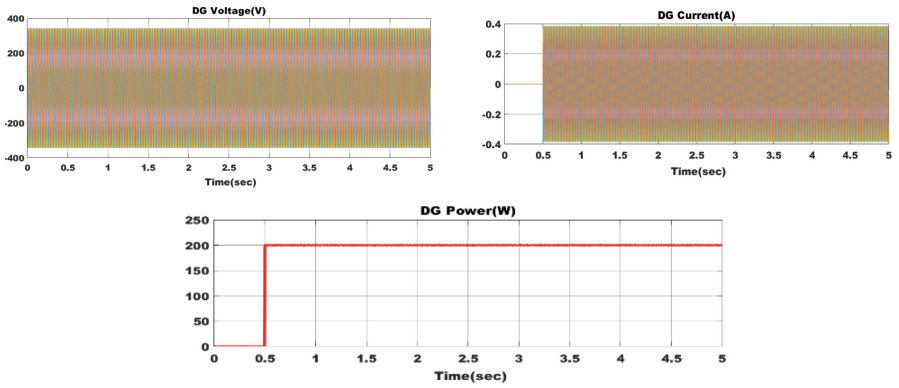


**Fig. 11.** Diesel generator performance when the load is reduced.

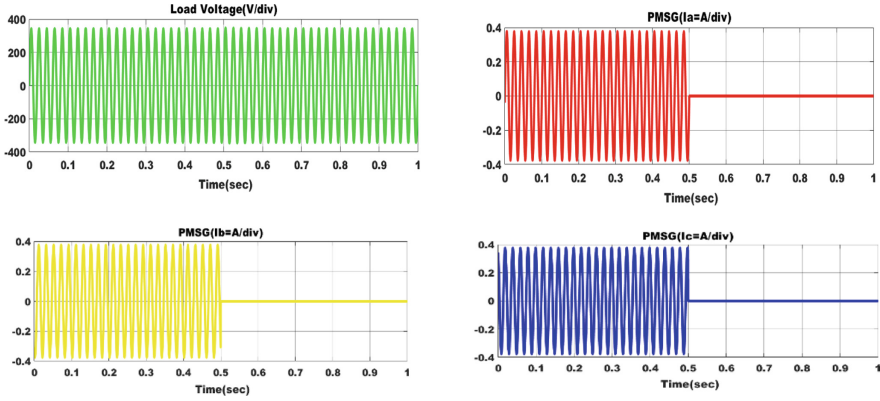


**Fig. 12.** When operating conditions are disconnected from the microgrid, the wind generator’s performance is assessed.

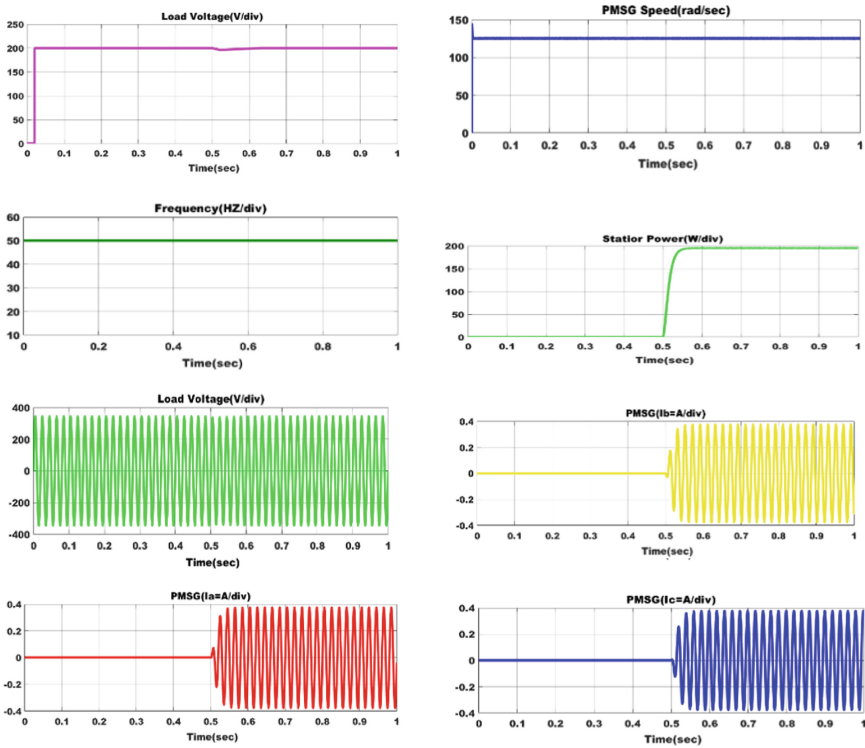


**Fig. 13.** Under conditions of reconnecting to the microgrid, the wind generator’s performance is assessed.

## 5 Conclusion

Using MATLAB/Simulink, the control and operation of a qZSC-based renewable hybrid microgrid was verified. Power sources for the proposed microgrid include solar, wind, and diesel generator. For the PV system, it is now possible to achieve MPP with reduced power oscillation because the performance of the SEPIC converter with the MPRVS-based P&O MPPT was successfully validated. Under various operating conditions Performance of the QZsi has been evaluated, and with swift dc-link voltage regulation it has been discovered to have better boost/buck characteristics. Hybrid wind, PV, and diesel application's dependability, output power quality, and efficiency in a microgrid the proposed QZsi design enhanced. The efficiency of the proposed strategy in dynamic conditions, such as abrupt changes in solar radiation or wind speed, by demonstrating that the optimal power has been monitored using renewable PV, wind, and diesel generator energy.

## References

1. "Fossil fuel production 'dangerously out of sync' with climate change targets IUNNews." <https://news.un.org/en/story/2021/10/1103472>.
2. P. Wang, J. Xiao, C. Jin, X. Han, and W. Qin, "Hybrid AC/DC Micro-Grids: Solution for High Efficient Future Power Systems," 2017, pp. 23–40.
3. M. Zolfaghari, G. B. Gharehpetian, M. Shafiekhah, and J. P. S. Catalão, "Comprehensive review on the strategies for controlling the interconnection of AC and DC microgrids," *International Journal of Electrical Power & Energy Systems*, vol. 136, p. 107742, Mar. 2022
4. T. Rajaraman, "Design and Implementation of Quazi-Z Source Inverter for AC Microgrid using Renewable Energy Source," *International Journal for Research in Applied Science and Engineering Technology*, vol. 6, no. 5, pp. 1737–1746, May 2018.
5. A. J. Lampião, T. Senjyu, and A. Yona, "Control of an autonomous hybrid microgrid as the energy source for a small rural village," *International Journal of Electrical and Computer Engineering*, vol. 7, no. 1, pp. 86–99, 2017.
6. S. D. Veeraganti and R. Nittala, "Operation of Microgrid and Control Strategies," 2019, pp. 434–449.
7. N. M. Dawoud, T. F. Megahed, and S. S. Kaddah, "Enhancing the performance of multi-microgrid with high penetration of renewable energy using modified droop control," *Electric Power Systems Research*, vol. 201, p. 107538, Dec. 2021.
8. Y. P. Siwakoti, F. Z. Peng, F. Blaabjerg, P. C. Loh, and G. E. Town, "Impedance-Source Networks for Electric Power Conversion Part I: A Topological Review," *IEEE Transactions on Power Electronics*, vol. 30, no. 2, pp. 699–716, Feb. 2015
9. X. Zhu, B. Zhang, and D. Qiu, "Enhanced boost quasi-Z- source inverters with active switched-inductor boost network," *IET Power Electronics*, vol. 11, no. 11, pp. 1774–1787, Sep. 2018.
10. Y. Li, S. Jiang, J. G. Cintron-Rivera, and F. Z. Peng, "Modeling and Control of Quasi-Z-Source Inverter for Distributed Generation Applications," *IEEE Transactions on Industrial Electronics*, vol. 60, no. 4, pp. 1532–1541, Apr. 2013.
11. A. O. AsSakka, M. A. ElShahed, M. A. Moustafa Hassan, and T. Senjyu, "Modeling and control of a PV based QZSI for grid-connected applications," in 2017 International Conference on Control, Automation and Information Sciences (ICCAIS), Oct. 2017, pp. 67–72.
12. L. Monjo, L. Sainz, J. J. Mesas, and J. Pedra, "Quasi-Z-Source Inverter-Based Photovoltaic Power System Modeling for Grid Stability Studies," *Energies*, vol. 14, no. 2, p. 508, Jan. 2021.

13. I. Grgic, M. Basic, D. Vukadinovic, and M. Bubalo, “Optimal Control of a Standalone Wind-Solar-Battery Power System with a Quasi-Z-Source Inverter,” in 2020 9th International Conference on Renewable Energy Research and Application (ICRERA), Sep. 2020, pp. 61–66.
14. M. Raja Nayak, V. V. K. Tulasi, K. Divya Teja, K. Koushic, and B. Suresh Naik, “Implementation of quasi-Z-source inverter for renewable energy applications,” *Materials Today: Proceedings*, Jul. 2021.
15. D. Sun, L. Du, X. Lu, and L. He, “An Energy-Stored Quasi-Z Source Converter Based Inter-linking Converter for Hybrid AC/DC Microgrids,” in IECON 2018 - 44th Annual Conference of the IEEE Industrial Electronics Society, Oct. 2018, pp. 3821–3826.
16. N. Priyadarshi, S. Padmanaban, D. Ionel, L. Mihet-Popa and F. Hybrid PV-Wind Azam, “Micro-Grid Development Using Quasi-Z-Source Inverter Modeling and Control—Experimental Investigation”, *Energies*, vol. 11, p. 2277, 2018.

**Open Access** This chapter is licensed under the terms of the Creative Commons Attribution-NonCommercial 4.0 International License (<http://creativecommons.org/licenses/by-nc/4.0/>), which permits any noncommercial use, sharing, adaptation, distribution and reproduction in any medium or format, as long as you give appropriate credit to the original author(s) and the source, provide a link to the Creative Commons license and indicate if changes were made.

The images or other third party material in this chapter are included in the chapter’s Creative Commons license, unless indicated otherwise in a credit line to the material. If material is not included in the chapter’s Creative Commons license and your intended use is not permitted by statutory regulation or exceeds the permitted use, you will need to obtain permission directly from the copyright holder.

